THERMODYNAMIC AND THERMOECONOMIC EVALUATION AND OPTIMIZATION OF AN ORC COUPLED TO A COMBINED REVERSE OSMOSIS/MEMBRANE DISTILLATION DESALINATION SYSTEM

Ammar Mouaky[1,2]*, Adil Rachek[2,3]

[1]Green Energy Park (IRESEN, UM6P), Solar Thermal Department, Benguerir, Morocco

[2]Ecole Mohammadia d'Ingénieurs-Mohammed V University, TRE Research Team, Rabat, Morocco

[3]National School of Mines of Rabat, Department of Process Engineering, Rabat, Morocco

*Corresponding Author: ammar.mouaky@gmail.com

ABSTRACT

This paper aims to evaluate and optimize the exergy and exergoeconomic performances of a 100 kW_e ORC block coupled to a combined reverse osmosis/membrane desalination (MD) system to meet the electricity, hot water, and freshwater requirements for a remote inland community. The studied plant's configuration includes a hybrid solar/biomass heat generation system feeding an ORC cycle. Depending on the end-users' electricity load demand, part of the produced electricity can be used to drive a reverse osmosis unit for brackish water desalination. On the other hand, a fraction of the heat rejected from the ORC condenser is recovered to meet the community's hot water requirements and to feed a membrane distillation unit used to minimize the brine liquid discharge rejected by the reverse osmosis process. Optimization studies based on genetic algorithms were conducted at design conditions to evaluate the impact of the ORC working fluid, its operating conditions, and the hot source temperature on the ORC exergy efficiency, hourly exergoeconomic cost of the produced useful outputs, and the membrane distillation permeate production. Besides, parametric studies were conducted to evaluate the impact of biomass cost, main plant's components costs, and the solar field's aperture on the investigated system's performances. Results showed that R245-fa allows achieving the optimal ORC exergy efficiency and MD permeate production, whereas R1336mzz(Z) permits reaching the minimum overall exergoeconomic cost. Results also showed that for the case of R245-fa, increasing the hot source temperature has a positive impact on the plant's performances. According to the parametric studies results, biomass cost and ORC investment cost are the most influencing cost items on the hourly exergoeconomic cost of the system. Parametric studies also showed that the increase of the solar field aperture from 1106.4 to 3319.2 m² leads to a rise of the overall exergoeconomic cost by up to 29.87%.

1 INTRODUCTION

Water availability can be considered a global challenge as about 5 billion people live in regions where water security is an issue (Rodell *et al.*, 2018) . In Africa, almost 600 million people are threatened by water scarcity, which severely affects local populations' living conditions and represents a real barrier to the socio-economic development for many African countries (Okoye and Oranekwu-Okoye, 2018; Rodell *et al.*, 2018). This situation is expected to be exacerbated by climate change, population growth, and dwindling resources (Okoye and Oranekwu-Okoye, 2018). In this regard, water desalination is increasingly proving to be a viable solution for supplying freshwater needs for different applications and in different regions in the world. This is mainly due to the technological advances recorded over the past two decades in this sector, particularly in reverse osmosis (RO) technology, where the cost of treated water has now reached competitive prices (World Bank, 2019). However, desalination technologies still face some challenges, including the management of brine discharges obtained after treatment, particularly for the case of inland brackish water desalination. On the other hand, the electricity supply is another challenge to be tackled in Africa, where 47% of the population still lacks

electricity access. The problem is particularly pronounced in Sub-Saharan countries where the electrification rate is only 32% (Okoye and Oranekwu-Okoye, 2018). Decentralized systems co-producing freshwater and electricity appear to be a viable option to address electricity and freshwater security challenges in such a context. In this regard, several system's configurations were investigated in the literature. (Leiva-Illanes *et al*., 2017)) investigated the exergoeconomic performances of a polygeneration system comprising a multi-effect desalination unit driven by solar energy in Chile. Hoffmann and Dall (2018) evaluated the performances of a solar plant co-producing electricity and desalinated water for a community and mining operations in Namibia. Mouaky and Rachek (2020a, 2020b) evaluated the exergetic and exergoeconomic performances of a hybrid solar/biomass system in Morocco, co-producing several useful outputs, including electricity, freshwater, and hot water. In this paper, a novel configuration of a hybrid solar/biomass system producing similar outputs and coupled to a membrane distillation (MD) unit for RO brine minimization is proposed. The main novelty of the present work compared to the mentioned studies is the inclusion of an additional process (MD) feed by part of the rejected heat from the ORC to minimize the final brine discharge volume rejected by the plant. The proposed configuration is optimized and evaluated through investigating the impact of the ORC working fluid, hot source temperature, biomass and plant's components capital costs, and solar field aperture on the plant's exergy and exergoeconomic indicators.

2 PLANT DESCRIPTION

The studied plant's configuration is represented in Figure 1. The plant includes four main circuits:

- Heat transfer (HTF) circuit: it consists of a hybrid heat generation system combining a compound parabolic collectors' (CPC) solar field and a biomass boiler arranged in series,
- ORC circuit: the heat produced by the HTF circuit is transferred through three heat exchangers (preheater, evaporator, and superheater) to the ORC circuit. After the expansion of the working fluid vapor at the turbine, the expanded vapor is condensed on a hybrid (air/water) condenser. Hence, when operated under the wet mode (water is used as a cooling medium), the rejected heat from the ORC circuit is recovered to produce hot water,
- RO circuit: Part of the plant's produced electricity is used to drive an RO unit during off-peak electricity demand periods. A fraction of the produced freshwater is used directly to meet the requirements of the end-users, whereas the remaining part is used to produce domestic hot water and to condensate the water vapor at the MD unit,
- MD circuit: The rejected brine from the RO unit is treated on the MD circuit. This block aims to minimize the discharged liquid volume feeding the evaporation pond, and to recover an additional amount of freshwater, using a membrane distillation system fed by a fraction of the rejected heat from the ORC circuit.

The studied plant was co-simulated using Ebsilon Professional® (STEAG Energy services GmbH, 2014) and the Water Application Value Engine (WAVE) software (WAVE Software for Water Treatment Plant Design). The solar field and the MD unit were modeled using experimental results (Liu *et al*., 2017; Osório *et al*., 2019) and coupled to Ebsilon Professional's built-in components using the "Programmable component", whereas WAVE was used to model the RO unit. Table 1 summarizes the main parameters considered for the simulations.

Table 1: Main considered parameters for the simulation

Parameter	Value
CPC concentration ratio	2.5
Heat transfer fluid (HTF)	Therminol-VP1
Working fluids	R245-fa, R1234ze(Z), R1233zd(E), R1336mzz(Z)
ORC capacity, kW	100
Turbine isentropic efficiency, %	75
Pumps isentropic efficiency	70
Brackish water total dissolved solids, mg/L	2160 (Gourai, 2018)
MD membranes surface, m²	50

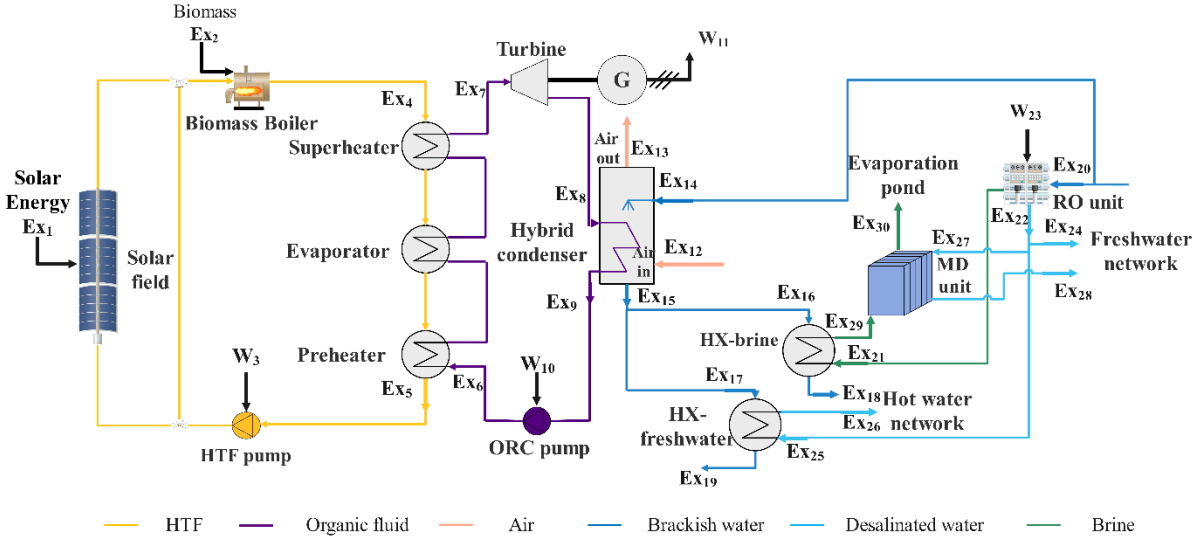

Figure 1: Plant's configuration

3 PLANT'S EXEREGETIC AND EXERGOECONOMIC ANALYSIS

Plant's optimization and evaluation were conducted using an approach combining exergy and exergoeconomic indicators. Optimization is conducted assuming design conditions (i.e., system's components are operated continuously at full load).

Plant's optimization was conducted considering the objective functions presented in Equation (1):

$$\begin{cases} \boldsymbol{max\ \eta_{ex,ORC}} : maximize\ the\ ORC\ circuit\ exergy\ efficiency \\ \boldsymbol{max\ J} : maximize\ the\ permeate\ (freshwater) recovery\ from\ the\ MD\ unit \\ \boldsymbol{min\ Z_{ex,overall}} : minimize\ the\ hourly\ exergoeconomic\ cost\ of\ the\ plant \end{cases} \quad (1)$$

Where the ORC circuit exergy efficiency ($\eta_{ex,ORC}$) is evaluated using the following equation:

$$\eta_{ex,ORC} = \frac{(\dot{W}_{11} - \dot{W}_{10}) + (\dot{E}x_{15} - \dot{E}x_{14})}{\dot{E}x_4 - \dot{E}x_5} \quad (2)$$

The overall hourly exergoeconomic cost of the produced useful outputs ($Z_{ex,overall}$) is calculated according to Equation (3):

$$Z_{ex,overall} = (c_{11} \cdot \dot{W}_{11}) + (c_{24} \cdot \dot{E}_{24}) + (c_{26} \cdot \dot{E}_{26}) + (c_{28} \cdot \dot{E}_{28}) \quad (3)$$

Where the hourly exergy rates ($\dot{E}_i$), hourly electricity rates ($\dot{W}_j$) and unit exergy costs (c_x) mentioned in Equations (2) and (3) are associated to Figure 1.

Table 2 summarizes the used balance equation and auxiliary relations to evaluate the unit costs of the produced useful outputs.

The non-exergetic related costs for the different equipment $\dot{Z}_k$ are calculated using Equation (4):

$$\dot{Z}_k = \frac{I_k \cdot crf}{\tau_k} + \frac{O\&M_k}{\tau_k} \quad (4)$$

Table 2: Balance equations and auxiliary relations of the exergoeconomic model

Block	Balance equation	Auxiliary relations
HTF circuit	$c_4 \cdot \dot{E}x_4 = c_1 \cdot \dot{E}x_1 + c_2 \cdot \dot{E}x_2 + c_3 \cdot \dot{W}_3 + c_5 \cdot \dot{E}x_5 + \dot{Z}_{HTF}$	$c_1 = 0; c_3 = c_{11}$
HXs-ORC circuit	$c_7 \cdot \dot{E}x_7 + c_5 \cdot \dot{E}x_5 = c_6 \cdot \dot{E}x_6 + c_4 \cdot \dot{E}x_4 + \dot{Z}_{HXs}$	$c_4 = c_5$
Turbine-ORC	$c_{11} \cdot \dot{W}_{11} + c_8 \cdot \dot{E}x_8 = c_7 \cdot \dot{E}x_7 + \dot{Z}_{Turbine}$	$c_8 = c_7$
Hybrid condenser	$c_{13} \cdot \dot{E}x_{13} + c_{15} \cdot \dot{E}x_{15} + c_9 \cdot \dot{E}x_9 = c_8 \cdot \dot{E}x_8 + c_{12} \cdot \dot{E}x_{12} + c_{14} \cdot \dot{E}x_{14} + \dot{Z}_{cond}$	$c_8 = c_9$; $c_{12} = 0$; $c_{14} = 0$
Pump-ORC	$c_6 \cdot \dot{E}x_6 = c_9 \cdot \dot{E}x_9 + c_{10} \cdot \dot{W}_{10} + +\dot{Z}_{Pump}$	$c_{10} = c_{11}$
RO unit	$c_{21} \cdot \dot{E}x_{21} + c_{22} \cdot \dot{E}x_{22} = c_{20} \cdot \dot{E}x_{20} + c_{23} \cdot \dot{W}_{23} + \dot{Z}_{RO}$	$c_{23} = c_{11}; c_{20} = 0$ $c_{21} = 0$
MD unit	$c_{28} \cdot \dot{E}x_{28} + c_{30} \cdot \dot{E}x_{30} = c_{27} \cdot \dot{E}x_{27} + c_{29} \cdot \dot{E}x_{29} + \dot{Z}_{MD}$	$c_{27} = c_{22}$
HX-Brine	$c_{18} \cdot \dot{E}x_{18} + c_{29} \cdot \dot{E}x_{29} = c_{16} \cdot \dot{E}x_{16} + c_{21} \cdot \dot{E}x_{21} + \dot{Z}_{HX-Brine}$	$c_{16} = c_{15}$
HX-Freshwater	$c_{19} \cdot \dot{E}x_{19} + c_{26} \cdot \dot{E}x_{26} = c_{17} \cdot \dot{E}x_{17} + c_{26} \cdot \dot{E}x_{26} + \dot{Z}_{HX-Freshwater}$	$c_{17} = c_{15}$; $c_{25} = c_{22}$

Where I_k, $O\&M_k$ and τ_k are respectively the investment cost, the operation and maintenance cost and the number of hours of operation at nominal conditions associated to the kth component, and crf is the capital recovery factor.
The assumed values for $O\&M_k$, τ_k and crf are provided in Table 3, whereas the investment cost is either evaluated considering the assumptions provided in Table 3 (HTF circuit, RO and MD units) or considering Equation (5) (Turton *et al.*, 2008) for the other components:

$$I_k = \frac{CEPCI_{2019} \cdot C_{BM2001}}{CEPCI_{2001}} \tag{5}$$

Where $CEPCI_{2001}$ and $CEPCI_{2019}$ are respectively the chemical engineering plant cost index for the years 2001 and 2019 and C_{BM2001} is the bare module cost for the considered equipment in 2001, evaluated using Equation (6):

$$C_{BM2001} = \begin{cases} C_p^0\left(B_1 + B_2 F_M F_p\right), & Heat\ exchangers\ and\ pumps \\ C_p^0 F_{BM} F_p\ , & Evaporator \\ C_p^0 F_{BM}\ , & Turbine \end{cases} \tag{6}$$

Where C_p^0 is the purchased cost for base conditions, B_1 and B_2 are the bare module factor constants, F_M is the material factor, F_p is the pressure factor and F_{BM} is the bare module factor.
C_p^0 and F_p are evaluated according to Equations (7) and (8) :

$$log_{10} C_p^0 = K_1 + K_2 log_{10}(A) + K_3 [log_{10}(A)]^2 \tag{7}$$

$$log_{10} F_p = C_1 + C_2 log_{10}(P) + C_3 [log_{10}(P)]^2 \tag{8}$$

Where K_1, K_2 and K_3 are the equipment cost data, A is the capacity or size parameter for the equipment, C_1, C_2 and C_3 are pressure factors and P is the operating pressure of the equipment.
Table 3 presents the considered assumptions of the cost estimations, whereas the values of the factors used in Equations (5) to (8) are provided in (Turton *et al.*, 2008).

Table 3: Main cost assumptions for the exergoeconomic model

Parameter	Value	Source
Solar field specific cost, €/m²	250	(Mouaky and Rachek, 2020b)
Biomass boiler specific cost, €/kW$_{th}$	300	(Malico *et al.*, 2019)
RO unit cost, €/m^3/day	184	(Nayar, 2020)
MD membranes specific cost, €/m²	103.5	(Tavakkoli *et al.*, 2017)
HTF circuit O&M cost, €/y	1% of the HTF circuit investment cost	Assumed
ORC circuit O&M cost, €/y	1% of the ORC block investment cost	Assumed
RO unit O&M cost	Maintenance cost: 0.18 €/m^3 Membrane replacement cost: 0.054 €/m^3 Chemicals cost: 0.054 €/m^3	(Maleki, 2018)
MD unit O&M cost	Maintenance cost :0.03 €/m^3 Membrane replacement: 20%/year Chemicals cost: 0.016 €/m^3	(Tavakkoli *et al.*, 2017)
Biomass cost (including transport), €/T	60	Local providers
ORC working fluids cost, €/kg	50	(Kosmadakis *et al.*, 2020)
HTF cost, €/kg	1.6	(Pili *et al.*, 2017)
Required quantity of ORC working fluid, kg	5050	(Collings *et al.*, 2016)
Required quantity of HTF, L	3000 + (50*number of solar field parallel lines)	(Wye Valley Energy)
	0.062 (assuming a lifetime of 20 years)	(BANK AL-MAGHRIB, 2020)
CEPCI$_{2001}$	397	(Turton *et al.*, 2008)
CEPCI$_{2019}$	609.3	(Unlu *et al.*, 2020)
τ_k, hours	8760	Assumed

4 RESULTS AND DISCUSSION

4.1 Working fluid comparison

Genetic algorithms-based optimization was conducted considering the working fluids and constraints mentioned in Table 4. The maximum pressure is varied between 8 bars and 90% of the critical pressure for each fluid (subcritical conditions), whereas the superheating degree is varied between 2 and 10 K, since superheating can be necessary even for dry fluids (Zhang *et al.*, 2018)

Optimization results are presented in Figure 2, whereas Table 5 presents the plant's operating conditions for the configurations allowing achieving the optimal exergy efficiency, exergoeconomic cost and MD production.

When considering the maximization of the ORC exergy efficiency and the MD permeate production, the results show that R245-fa is the optimal working fluid with an exergy efficiency and MD permeate production of respectively 58.95 % and 0.46 kg/s. On the other hand, the optimal overall hourly exergoeconomic cost (37.12 €/h) is reached when using R1336mzz(Z) as a working fluid. Optimization results showed that under the actual biomass and solar field specific costs, optimal results are achieved when operating the system without including a solar field.

Table 4: Considered working fluids and optimization constraints

Working fluid	R245-fa	R1234ze(Z)	R1233zd(E)	R1336mzz(Z)
High pressure of the ORC, bars	8 to 32.56	8 to 31.77	8 to 32.61	8 to 26.13
Low pressure of the ORC, bars	1 to 10			
Superheating degree, K	2 to 10			
Hot water temperature, °C	55			

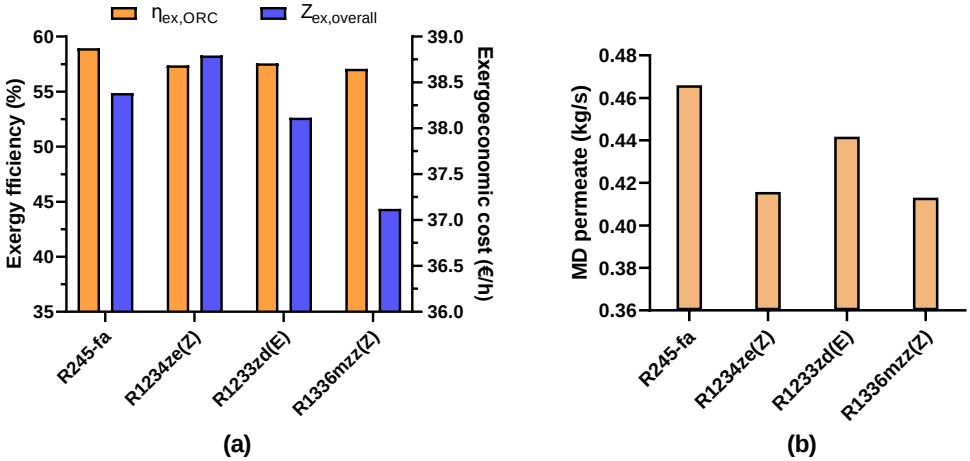

Figure 2: ORC working fluids optimization results: (a) exergy efficiency and total exergoeconomic cost, (b) MD permeate

Table 5: Plant's operating conditions for the optimal configurations

	Exergy efficiency	Exergoeconomic cost	MD permeate
Biomass boiler capacity, kW	1190	892	1214
ORC pressures (high/low), bars	31.114/10	21.824/3.257	30.166/10
Superheating degree, K	2	10	2
Heat exchangers surfaces, m²			

To allow a multi-objective comparison of the considered working fluid, a fourth objective function is defined in Equation (9) as function of the values plotted in Figure 2:

$$M_{WF} = \left(\alpha \cdot \frac{\eta_{ex,ORC,WF} - \min(\eta_{ex,ORC})}{\max(\eta_{ex,ORC}) - \min(\eta_{ex,ORC})}\right) + \left(\beta \cdot \frac{J_{WF} - \min(J)}{\max(J) - \min(J)}\right) + \left(\gamma \cdot \frac{Z_{ex,overall,WF} - \max(Z_{ex,overall})}{\min(Z_{ex,overall}) - \max(Z_{ex,overall})}\right) \quad (9)$$

Where α, β and γ are respectively the weight factors related to ORC exergy efficiency, MD production and overall exergoeconomic cost. Figure 3 presents the results obtained for the four scenarios shown in Table 6:

Table 6: Weight factors values for the considered scenarios

Scenarios	α	β	γ
1	$\frac{1}{2}$	$\frac{1}{2}$	0
2	$\frac{1}{2}$	0	$\frac{1}{2}$
3	0	$\frac{1}{2}$	$\frac{1}{2}$
4	$\frac{1}{3}$	$\frac{1}{3}$	$\frac{1}{3}$

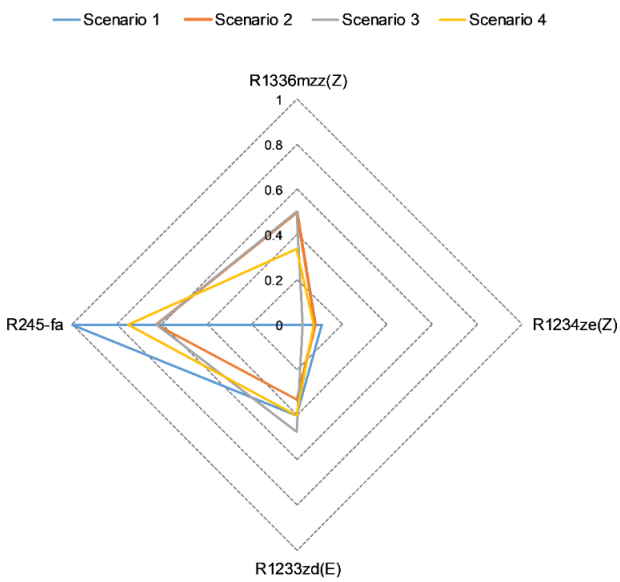

Figure 3: Multi-objective optimization results for the considered scenarios

As can be seen from Figure 3, R245-fa is the fluid having the optimal M_{WF} value for all considered scenarios with M_{WF} values varying between 1 (scenario 1) and 0.622 (scenarios 2 and 3). It is therefore considered as the working fluid for the ORC in the following subsections.

4.2 Hot source temperature impact

To evaluate the impact of the hot source temperature on the optimization results, a parametric study was conducted considering three values of the HTF temperature at the inlet of the superheater (170, 180, and 190°C). For each temperature, an optimization study of the three objective functions was conducted.

The parametric study results are illustrated in Figure 4. According to the figure, the increase of HTF inlet temperature from 170 to 190°C is associated with a reduction of the overall exergoeconomic cost from 38.55 to 38.3 €/h. The increase of the HTF inlet temperature between 170 and 180 also positively impacts the ORC exergy efficiency and MD permeate production. In contrast, it can be noticed from the figure that an increase of the HTF inlet temperature from 180 to 190°C provides a limited improvement of the exergy efficiency (58.95 to 59.21%) and practically no improvement on the MD permeate production. The limited impact of the HTF temperature increase from 180 to 190°C on the system's performances can be attributed to the combination of the constraint imposed in table 4 related

to the high pressure of the ORC and the fact that superheating is generally reducing the performances of ORC systems (Wang et al., 2018).

4.3 Main plant's components and biomass costs impact

The variation of produced useful outputs hourly costs as a function of the biomass specific cost and the capital costs of the ORC circuit, the HTF circuit, and the RO unit are represented in Figure 5 (using R245-fa as a working fluid and considering the optimal exergoeconomic cost configuration). As can be seen from the figure, the variation of the biomass cost significantly impacts the overall exergoeconomic cost of the produced outputs. Indeed, an increase of the biomass specific cost from 60 to 72 €/T leads to an increase from 3.18% (MD water) to 11.68% (electricity) of the specific cost of the produced outputs. On the other hand, an increase by 20% of the ORC circuit capital cost induces an increase of 5.08% of the overall exergoeconomic cost. In contrast, the HTF circuit and RO unit capital costs have a lower influence on the plant's overall exergoeconomic cost.

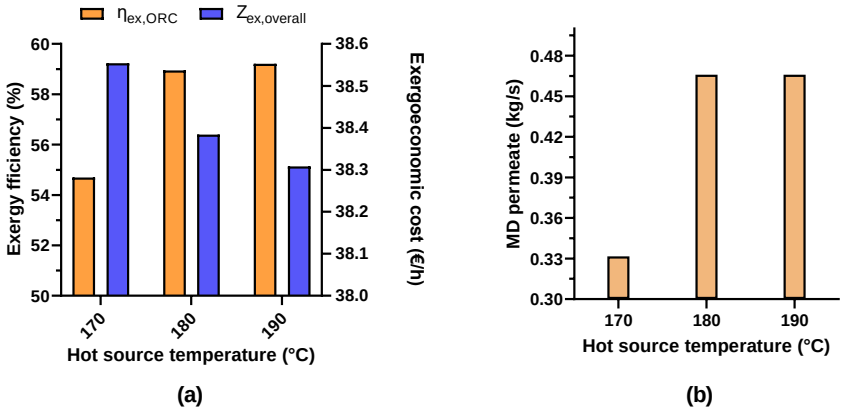

Figure 4: Hot source temperature impact on the considered objective functions (R245-fa)

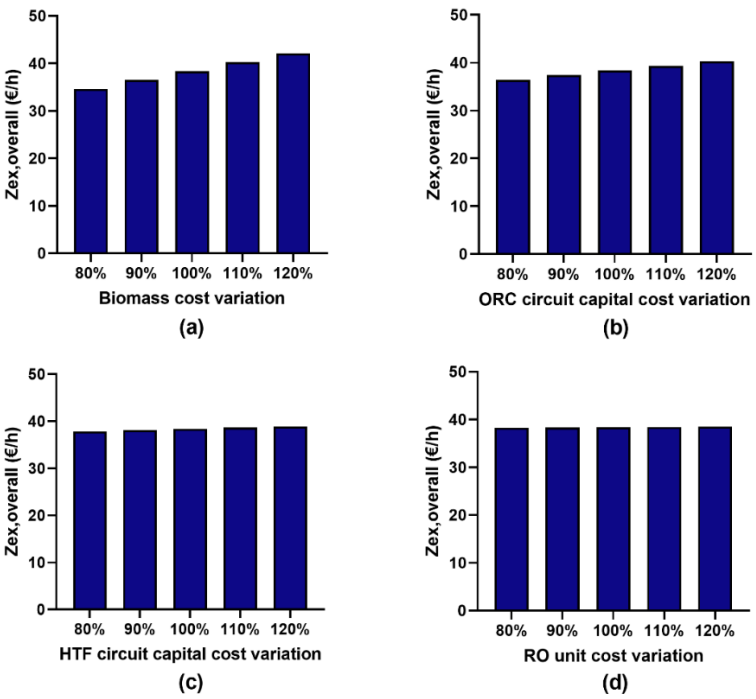

Figure 5: Biomass and main plant's components costs variation impact on the overall exergoeconomic cost: (a) Biomass cost, (b) ORC circuit capital cost, (c) HTF circuit capital cost, (d) RO unit cost

4.4 Solar field's aperture impact

Table 7 illustrates the solar field's aperture impact on the overall exergoeconomic cost of the plant (under the same conditions of subsection 4.3). Calculations were performed for two cases: a first case where the CO_2 emissions originating from the biomass combustion are not subject to taxes (case 1) and a second case where a tax of 60€/TCO_{2eq} (World Bank and Ecofys, 2018) is assumed (case 2). As shown in the table, the increase of the solar aperture from 1106.4 to 3319.2 m² leads to an improvement of the solar share (ratio of the solar field's contribution to the total heat provided by the HTF circuit) from 7.97 to 21.75%. In contrast and given the actual solar field and biomass cost figures, the solar field aperture increase is accompanied by an overall exergoeconomic cost rise of 29.87 and 26.81% for the case 1 and case 2, respectively.

Table 7: Solar field's aperture impact on the overall exergoeconomic cost

Solar field aperture, m²	Solar share, %	$Z_{ex,overall}$, €/h	
		Case 1	Case 2
1106.4	7.97	44.73	48.06
1844	12.88	49.05	52.20
2581.6	17.47	53.455	56.45
3319.2	21.75	58.09	60.96

5 CONCLUSIONS

In this work, a hybrid solar/biomass system producing electricity, hot water, and freshwater was evaluated and optimized. The main conclusions of this work are as follows:

- R245-fa allows achieving the optimal ORC exergy efficiency and MD permeate production, whereas the optimal overall exergoeconomic cost is obtained using R1336mzz(Z),
- Increasing the HTF temperature at the inlet of the ORC superheater from 170 to 180°C has a significant impact on the plant's performances. On the other hand, the magnitude of improvement is lower from 180 to 190°C,
- The biomass specific cost, in addition to the ORC unit capital cost, have a significant impact on the plant's overall exergoeconomic cost,
- The solar share is tripled when increasing the solar field aperture from 1106.4 to 3319.2 m², however, this is accompanied by an increase of the exergoeconomic cost of up to 29.86%.

REFERENCES

BANK AL-MAGHRIB, 2020. REVUE MENSUELLE DE LA CONJONCTURE ÉCONOMIQUE, MONÉTAIRE ET FINANCIÈRE. BANK AL-MAGHRIB, Direction Etudes Economiques, Rabat.

Collings, P., Yu, Z., Wang, E., 2016. A dynamic organic Rankine cycle using a zeotropic mixture as the working fluid with composition tuning to match changing ambient conditions. Applied energy 171, 581–591.

Gourai, K., 2018. Osmose Inverse Alimentée par l'Énergie Solaire pour le Dessalement des Eaux Saumâtres et Tests d'Adsorption sur la Bentonite Activée (Doctoral thesis report).

Hoffmann, J.E., Dall, E.P., 2018. Integrating desalination with concentrating solar thermal power: A Namibian case study. Renewable Energy 115, 423–432. https://doi.org/10.1016/j.renene.2017.08.060

Kosmadakis, G., Arpagaus, C., Neofytou, P., Bertsch, S., 2020. Techno-economic analysis of high-temperature heat pumps with low-global warming potential refrigerants for upgrading waste heat up to 150° C. Energy Conversion and Management 226, 113488.

Leiva-Illanes, R., Escobar, R., Cardemil, J.M., Alarcón-Padilla, D.-C., 2017. Thermoeconomic assessment of a solar polygeneration plant for electricity, water, cooling and heating in high direct normal irradiation conditions. Energy Conversion and Management 151, 538–552. https://doi.org/10.1016/j.enconman.2017.09.002

Liu, J., Liu, M., Guo, H., Zhang, W., Xu, K., Li, B., 2017. Mass transfer in hollow fiber vacuum membrane distillation process based on membrane structure. Journal of Membrane Science 532, 115–123. https://doi.org/10.1016/j.memsci.2017.03.018

Maleki, A., 2018. Design and optimization of autonomous solar-wind-reverse osmosis desalination systems coupling battery and hydrogen energy storage by an improved bee algorithm. Desalination 435, 221–234.

Malico, I., Pereira, R.N., Gonçalves, A.C., Sousa, A.M., 2019. Current status and future perspectives for energy production from solid biomass in the European industry. Renewable and Sustainable Energy Reviews 112, 960–977.

Mouaky, A., Rachek, A., 2020a. Thermodynamic and thermo-economic assessment of a hybrid solar/biomass polygeneration system under the semi-arid climate conditions. Renewable Energy 156, 14–30. https://doi.org/10.1016/j.renene.2020.04.019

Mouaky, A., Rachek, A., 2020b. Energetic, exergetic and exergeoeconomic assessment of a hybrid solar/biomass poylgeneration system: A case study of a rural community in a semi-arid climate. Renewable Energy 158, 280–296. https://doi.org/10.1016/j.renene.2020.05.135

Nayar, K.G., 2020. Brackish water desalination for greenhouse agriculture: Comparing the costs of RO, CCRO, EDR, and monovalent-selective EDR. Desalination 475, 114188.

Okoye, C.O., Oranekwu-Okoye, B.C., 2018. Economic feasibility of solar PV system for rural electrification in Sub-Sahara Africa. Renewable and Sustainable Energy Reviews 82, 2537–2547.

Osório, T., Pereira, R., Coelho, A., Marchã, J., Pereira, J., Silva, R., Eusébio, T., Collares-Pereira, M., 2019. A novel quasi-stationary CPC-type solar collector for intermediate temperature range applications for process heat: Simulation and experimental results. Presented at the SOLARPACES 2018: International Conference on Concentrating Solar Power and Chemical Energy Systems, Casablanca, Morocco, p. 150006. https://doi.org/10.1063/1.5117662

Pili, R., Romagnoli, A., Spliethoff, H., Wieland, C., 2017. Techno-economic analysis of waste heat recovery with ORC from fluctuating industrial sources. Energy procedia 129, 503–510.

PRO 175-1,000kW Biomass Boilers - Wye Valley Energy [WWW Document], n.d. URL http://www.wyevalleyenergy.co.uk/products/boiler/pro-175-1000kw-biomass-boilers (accessed 7.1.21).

Rodell, M., Famiglietti, J.S., Wiese, D.N., Reager, J.T., Beaudoing, H.K., Landerer, F.W., Lo, M.-H., 2018. Emerging trends in global freshwater availability. Nature 557, 651–659. https://doi.org/10.1038/s41586-018-0123-1

STEAG Energy services GmbH, 2014. Ebsilon Professional.

Tavakkoli, S., Lokare, O.R., Vidic, R.D., Khanna, V., 2017. A techno-economic assessment of membrane distillation for treatment of Marcellus shale produced water. Desalination 416, 24–34.

The Role of Desalination in an Increasingly Water-Scarce World [WWW Document], n.d. URL https://openknowledge.worldbank.org/handle/10986/31416 (accessed 5.3.21).

Turton, R., Bailie, R.C., Whiting, W.B., Shaeiwitz, J.A., 2008. Analysis, synthesis and design of chemical processes. Pearson Education.

Unlu, S., Niu, W., Demirel, Y. ar, 2020. Bio-based adipic acid production: feasibility analysis using a multi-criteria decision matrix. Biofuels, Bioproducts and Biorefining 14, 794–807.

Wang, D., Ma, Y., Tian, R., Duan, J., Hu, B., Shi, L., 2018. Thermodynamic evaluation of an ORC system with a low pressure saturated steam heat source. Energy 149, 375–385.

WAVE Software for Water Treatment Plant Design [WWW Document], n.d. URL https://www.dupont.com/water/resources/design-software.html (accessed 11.22.19).

World Bank and Ecofys, 2018. State and Trends of Carbon Pricing 2018 (May).

Zhang, C., Liu, C., Xu, X., Li, Q., Wang, S., Chen, X., 2018. Effects of superheat and internal heat exchanger on thermo-economic performance of organic Rankine cycle based on fluid type and heat sources. Energy 159, 482–495.

Wye Valley Energy URL http://www.wyevalleyenergy.co.uk/products/boiler/pro-175-1000kw-biomass-boilers.